Petroleum Science 19 (2022) 3080–3087

Contents lists available at ScienceDirect

Petroleum Science

journal homepage: www.keaipublishing.com/en/journals/petroleum-science

Original Paper

Novel CoAl-LDH Nanosheets/$BiPO_4$ nanorods composites for boosting photocatalytic degradation of phenol

Ya-Jun Wang [a, 1, *], Jia-Ying Zhang [a, 1], Shuang-Shuang Hou [a], Jia-Xing Wu [a], Cong Wang [a], Yu-Ming Li [a], Gui-Yuan Jiang [a, **], Guo-Qing Cui [a]

[a] State Key Laboratory of Heavy Oil Processing, China University of Petroleum, Beijing, 102249, China

ARTICLE INFO

Article history:
Received 30 October 2021
Received in revised form
28 December 2021
Accepted 7 January 2022
Available online 19 January 2022

Edited by Xiu-Qiu Peng

Keywords:
$BiPO_4$
CoAl-LDH
Photocatalytic degradation
Phenol

ABSTRACT

Layered double hydroxide (LDH) with special layered structure has been proved to have excellent hole transport capacity and good stability. Herein, we report a high efficient composite photocatalyst of CoAl-LDH and $BiPO_4$ prepared by hydrothermal and chemical adsorption (denoted as CoAl-LDH/$BiPO_4$). Phenol can be entirely degraded by 1% CoAl-LDH/$BiPO_4$ under 30 min ultraviolet (UV) light irradiation, and the degradation rate constants k are 3 times and 39 times higher than that of pure $BiPO_4$ and CoAl-LDH, respectively. The enhanced photocatalytic activity can be attributed to effective holes transfer from $BiPO_4$ to CoAl-LDH, which hinders the recombination of photogenerated charge carriers. In addition, the combination of $BiPO_4$ and CoAl-LDH avoids the agglomeration of $BiPO_4$ and improves the stability of $BiPO_4$. Active species capture experiments indicate that superoxide radicals ($\cdot O_2^-$) are the main active species responsible for the degradation of phenol. This work provides technical approaches and research ideas for solving the photogenerated charge carrier recombination problem of photocatalyst.

1. Introduction

With the increase of world population and the development of industry, the environmental pollution is becoming more serious (Naciri et al., 2020; Gao et al., 2019; Bacha et al., 2019; Shekofteh et al., 2018; Zheng et al., 2010). In recent years, photocatalytic oxidation technology has been studied in the field of environment because of its high mineralization ability and no secondary pollution (Wang et al., 2020; Shi et al., 2020; Pellegrino et al., 2020; Yu et al., 2018; Chen et al., 2020; Chong et al., 2010). As a new photocatalyst, $BiPO_4$ possesses stable, nontoxic and robust oxidation ability, and its photocatalytic activity is better than TiO_2 (P25), which is expected to be used in water treatment (Di et al., 2017; Yi et al., 2019). Moreover, $BiPO_4$ shows excellent activity in degradation of various organic pollutants of dyes, phenols, benzenes, drugs, and polystyrene films under UV light (Liu et al., 2013; Zou et al., 2017; Guo et al., 2018). However, $BiPO_4$ also has disadvantages, such as wide bandgap (Eg = 3.8 eV), high charge recombination rate, and low quantum efficiency (Pan and Zhu, 2015; Vadivel et al., 2016). Therefore, improving the photogenerated charge separation efficiency of $BiPO_4$ has become the focus of researchers. Many methods have been employed to enhance the photocatalytic performance of $BiPO_4$, for instance, doping (Huang et al., 2013; Wang et al., 2018), heterojunction construction (Su et al., 2018; Ding et al., 2018; Cao et al., 2013; Mu et al., 2021) and surface hybridization (Wang et al., 2021).

Layered double hydroxides (LDHs) are a kind of two-dimensional anionic clay composed of the main layer of positive charge and the exchangeable intermediate anions (Wang and O'hare, 2012; Fang and Evana, 2014). Owing to their unique layered structure, LDHs can promote the transport of photogenerated carriers while avoiding nanoparticles agglomeration (Kumar et al., 2017; Dou et al., 2015; Gong and Dai, 2015; Zeng et al., 2020; Wan and Surendar, 2019). Compared with MgAl-LDH and ZnAl-LDH, CoAl-LDH can meet the thermodynamic requirements of generating free radicals and is an efficient photocatalyst for degradation of pollutants (Kumar et al., 2017). Santosh Kumar and co-workers prepared P25@CoAl-LDH nanocomposites for photocatalytic reduction of CO_2. P25 and CoAl-LDH formed a type II heterojunction, extending the utilization of the solar spectrum of

* Corresponding author. Yajun Wang
** Corresponding author. Guiyuan Jiang,
E-mail addresses: wangyajun@cup.edu.cn (Y.-J. Wang), jianggy@cup.edu.cn (G.-Y. Jiang).
[1] Yajun Wang and Jiaying Zhang contributed equally to this work.

https://doi.org/10.1016/j.petsci.2022.01.007

P25 (Santosh et al., 2017). Moreover, our group prepared NiFe-LDH/Bi_2WO_6 nanosheet arrays electrode by hydrothermal and electrochemical deposition methods and achieved excellent activity (Wang et al., 2021). Inspired by the previous work, the composite of $BiPO_4$ photocatalyst and CoAl-LDH with excellent hole transfer property may avoid the agglomeration of $BiPO_4$, enhancing the photocatalytic activity (Snehaprava et al., 2019; Lia et al., 2017; Santosh et al., 2018).

In this work, we successfully prepared CoAl-LDH/$BiPO_4$ by chemical adsorption. The ratio of CoAl-LDH and preparation temperature were investigated, to obtain an optimal composite catalyst. Phenol was chosen as a model pollutant to investigate the photocatalytic activity of CoAl-LDH/$BiPO_4$. Phenol can be completely degraded by 1% CoAl-LDH/$BiPO_4$ in 30 min, and the degradation rate constants k are 3 times and 39 times higher than that of pure $BiPO_4$ and CoAl-LDH, respectively. The structure of CoAl-LDH/$BiPO_4$ and the mechanism of the improved photocatalytic performance were systematically investigated.

2. Experimental section

The Experimental Section details are shown in the Supporting Information.

3. Results and discussion

3.1. Catalysts Characterization

The crystal structure of $BiPO_4$, CoAl-LDH and 1% CoAl-LDH/$BiPO_4$ are measured by XRD (Fig. 1(a)). All diffraction peaks show monoclinic monazite phase of $BiPO_4$ (JCPDS No 80–0209) without any impurity phase. For pure CoAl-LDH, the typical diffraction peaks at $2\theta = 12.18°$, 24.31°, 35.96°, 39.15° and 47.22° can be indexed to the (003), (006), (009), (012) and (018) (JCPDS No. 51-0045). No impurity peaks are found in the 1% CoAl-LDH/$BiPO_4$, indicating that CoAl-LDH does not change the crystal structure of $BiPO_4$. The Raman spectra of samples are shown in Fig. S1. $BiPO_4$ presents seven major Raman peaks which are assigned to first order Bi–O stretching vibration (220 and 276 cm^{-1}), ν1 symmetric stretching (970 cm^{-1}), ν2 bending vibration (400 cm^{-1}), ν3 asymmetric stretching (1040 cm^{-1}) and ν4 stretching vibration (550 cm^{-1}) of PO_4^{3-} (Maisang et al., 2018). The Raman spectra of $BiPO_4$ is unchanged after CoAl-LDH combination. Moreover, no CoAl-LDH peak can be observed in 1% CoAl-LDH/$BiPO_4$ may be due to the low content of CoAl-LDH. The optical properties of $BiPO_4$, CoAl-LDH and 1% CoAl-LDH/$BiPO_4$ were characterized by UV–Vis DRS (Fig. 1(b)). The band gaps of samples were listed in Table S1. Mechanical mixture composite catalyst (denoted as 1% CoAl-LDH/$BiPO_4$ mechanical mixture) was prepared for comparison. The bandgap of $BiPO_4$ is about 3.85 eV, which can only absorb ultraviolet light. The CoAl-LDH absorbs visible light in 400–500 nm. Compared with CoAl-LDH, the light absorption of 1% CoAl-LDH/$BiPO_4$ increases in the ultraviolet region.

The morphology of $BiPO_4$, CoAl-LDH and 1% CoAl-LDH/$BiPO_4$ are investigated by SEM and HRTEM images (Fig. 2). As can be noticed from SEM images (Figs. S2(a and b)), the $BiPO_4$ presents a nanorod morphology with a length of 500–1000 nm. Subsequently, CoAl-LDH is a multilayer sheet structure with an average diameter of about 2 μm (Figs. S2(c and d)). It is found that $BiPO_4$ is dispersed on the CoAl-LDH sheet structure, indicating the two are successfully combined (Fig. S2 (e, f)). To further observe the internal structure of the samples, the HRTEM images of $BiPO_4$, CoAl-LDH and 1% CoAl-LDH/$BiPO_4$ are shown in Fig. 2. The lattice spacing of $BiPO_4$ is 0.328 nm, which corresponds to the (200) plane of monoclinic monazite $BiPO_4$ (Fig. 2(a and b)) (Zhu et al., 2017; Shi et al., 2018). The lattice spacing of CoAl-LDH is 0.27 nm, which can be attributed to (012) plane (Fig. 2(c)) (Dou et al., 2015). Fig. 2(d) further illustrates the uniform distribution of $BiPO_4$ on the surface of CoAl-LDH sheets. The specific surface area and pore size distribution data of the three catalysts are shown in Table S2. The specific surface area of $BiPO_4$ is unchanged after CoAl-LDH combination (Fig. S3).

3.2. Photocatalytic performance

The photocatalytic activity of $BiPO_4$, CoAl-LDH, various CoAl-LDH/$BiPO_4$ is appraised by photocatalytic degradation of phenol under UV light, as shown in Fig. 3. The apparent rate constant k of the CoAl-LDH/$BiPO_4$ presents a volcanic appearance. 1% CoAl-LDH/$BiPO_4$ possesses optimal photocatalytic performance, and the reaction rate constant k of its degradation of phenol reaches 0.17134min^{-1}, which is about 3 folds higher than that of pure $BiPO_4$ (0.06194 min^{-1}) (Fig. 3(a and b)). The improved activity may be contributed to the more efficient light utilization and the higher separation efficiency of photogenerated electrons and holes of CoAl-LDH/$BiPO_4$. However, it is found that the activity of 5% CoAl-LDH/$BiPO_4$ and 10% CoAl-LDH/$BiPO_4$ is lower than that of pure $BiPO_4$. This may be due to the high shading effect of CoAl-LDH which inhibits the UV light absorption of $BiPO_4$, resulting in the

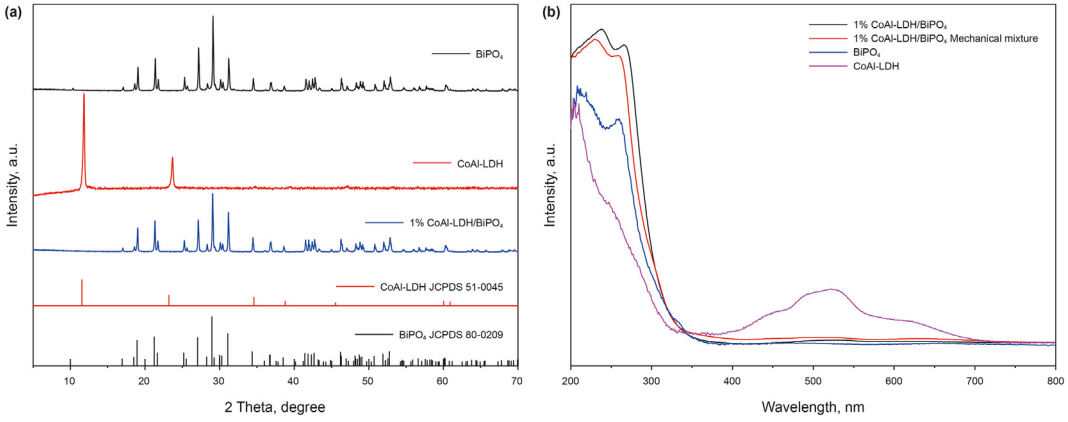

Fig. 1. **a** XRD patterns of $BiPO_4$, CoAl-LDH and 1% CoAl-LDH/$BiPO_4$; **b** UV–Vis DRS spectra of $BiPO_4$, CoAl-LDH, 1% CoAl-LDH/$BiPO_4$ and 1% CoAl-LDH/$BiPO_4$ mechanical mixture.

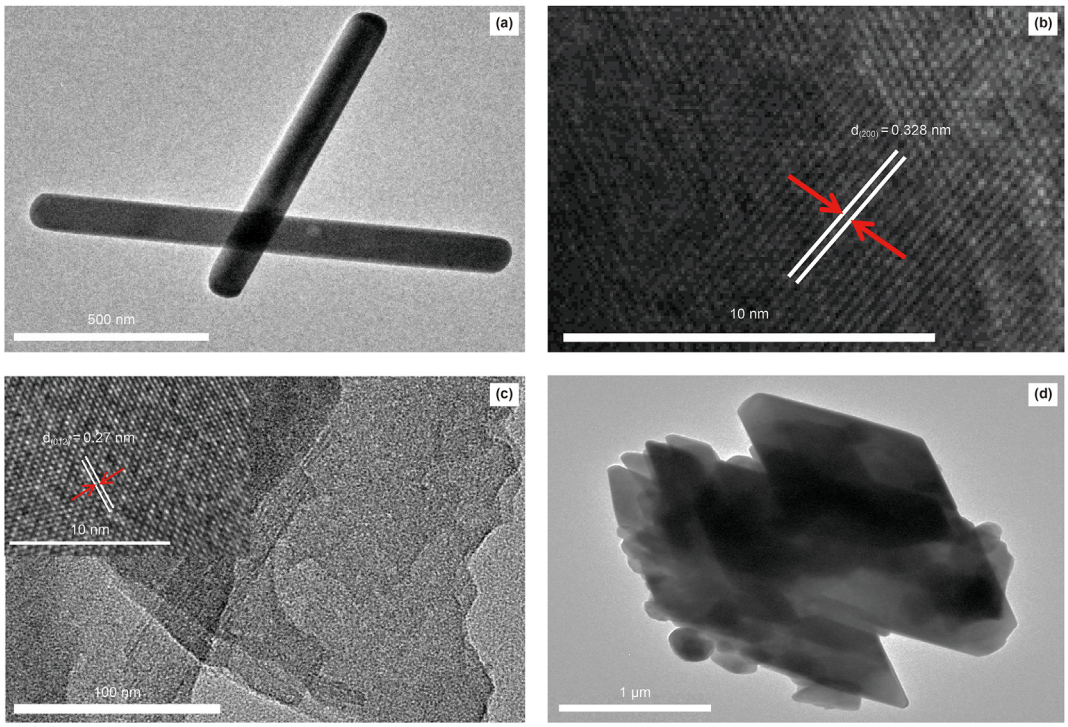

Fig. 2. HRTEM images of **a, b** $BiPO_4$; **c** CoAl-LDH; **d** 1% CoAl-LDH/$BiPO_4$.

decrease of $BiPO_4$ activity (Wang et al., 2011; Zhang et al., 2010). The effects of various preparation temperatures of CoAl-LDH/$BiPO_4$ on the degradation activity were also investigated, and the results were shown in Fig. 3(c and d). It is found that the optimal preparation temperatures is 50 °C.

The stability and reusability are important for the heterogeneous solid catalysts. The reusability of the 1% CoAl-LDH/$BiPO_4$ is evaluated by the three successive degradation cycles. As depicted in Fig. 3(e), the activity of 1% CoAl-LDH/$BiPO_4$ does not decrease significantly after three cycles. The above results show that the as-prepared 1% CoAl-LDH/$BiPO_4$ has excellent stability and reusability.

3.3. Mechanism of photocatalytic activity enhancement

To reveal the synergistic effect of CoAl-LDH and $BiPO_4$, a series of photocurrent tests are carried out on $BiPO_4$, CoAl-LDH and CoAl-LDH/$BiPO_4$. As shown in Fig. 4(a), 1% CoAl-LDH/$BiPO_4$ shows the highest photocurrent density under UV irradiation. To further prove the above results, electrochemical impedance spectroscopy (EIS) under UV irradiation is tested (Fig. 4(b)). The impedance radius of prepared samples under light condition are smaller than that under dark condition, suggesting that electrons and holes can be effectively separated under UV light irradiation (Chowdhury et al., 2018). The impedance radius of 1% CoAl-LDH/$BiPO_4$ is the smallest, indicating that the 1% CoAl-LDH/$BiPO_4$ has the optimal electron-hole separation efficiency. The above results are consistent with the results of phenol degradation, indicating that the synergistic effect between $BiPO_4$ and CoAl-LDH improves the separation efficiency of charge carriers.

XPS was used to investigate the chemical state of $BiPO_4$, CoAl-LDH and 1% CoAl-LDH/$BiPO_4$ (Fig. 5). As shown in Figs. 5(a), 1% CoAl-LDH/$BiPO_4$ contains Bi, P, Co, Al, C and O elements. The Bi 4f spectra (Fig. 5(b)) can be fitted to two discrete peaks at 159.5 eV and 164.8 eV, which are responded to Bi 4f $_{7/2}$ and Bi 4f $_{5/2}$ of $[Bi_2O_2]^{2+}$, indicating that the valence state of Bi atom is Bi^{3+} (Ji et al., 2009; Jiang et al., 2011; Diego et al., 2015). The Co 2p spectra (Fig. 5(c)) can be deconvoluted into two peaks at 781.2 eV and 796.6 eV, corresponding to Co 2p $_{3/2}$ and Co 2p $_{1/2}$, respectively. Moreover, the two companion peaks at 786.1 eV and 802.6 eV indicate the existence of highly spun bivalent Co^{2+} (Dou et al., 2015). After $BiPO_4$ and CoAl-LDH are compounded, the two Co 2p characteristic peaks shift positively to 786.7 eV and 805.5 eV, while the two Bi 4f characteristic peaks shift negatively to 159.1 eV and 164.1 eV, respectively. The increase of electron density of $BiPO_4$ and the decrease of electron density of CoAl-LDH can be attributed to the chemical interaction between $BiPO_4$ and CoAl-LDH, indicating the electron transfer from CoAl-LDH to $BiPO_4$ and the hole transfer from $BiPO_4$ to CoAl-LDH, thus improving the photogenerated charge separation efficiency of $BiPO_4$. For P 2p spectra (Fig. 5(d)), the peak at 132.9 eV is attributed to the pentavalent phosphorus-oxidation state (P^{5+}) of P—O bond in PO_4^{3-} (Guo et al., 2018).

To further verify the photocatalytic degradation mechanism of $BiPO_4$, CoAl-LDH and 1% CoAl-LDH/$BiPO_4$, it is necessary to conduct active species capture experiments, as shown in Fig. 6. The benzoquinone (BQ), methanol (CH_3OH) and tert-butyl alcohol (t-BuOH) are used to trap $\cdot O_2^-$, holes and $\cdot OH$, respectively (Zhu et al., 2017). As shown in Fig. 6(a and b), the main active species of $BiPO_4$ and CoAl-LDH degrading phenol are $\cdot O_2^-$. It can be noted from Fig. 6 (c) that after combined with CoAl-LDH, the active species in the degradation process of $BiPO_4$ is unchanged.

To sum up, the photocatalytic degradation mechanism of CoAl-LDH/$BiPO_4$ is speculated as follows (Fig. 7). Photogenerated electrons and holes are generated in CoAl-LDH/$BiPO_4$ under UV light irradiation. Photogenerated holes of $BiPO_4$ can quickly migrate to CoAl-LDH, thus improving the photogenerated charge separation efficiency. Moreover, CoAl-LDH can improve the reaction kinetics, resulting in an improved photocatalytic degradation activity (Wang and O'hare, 2012; Fang and Evana, 2014). Photogenerated electrons react with O_2 in the solution to form $\cdot O_2^-$, which is used to degrade pollutants in wastewater. Photogenerated holes transfer to the

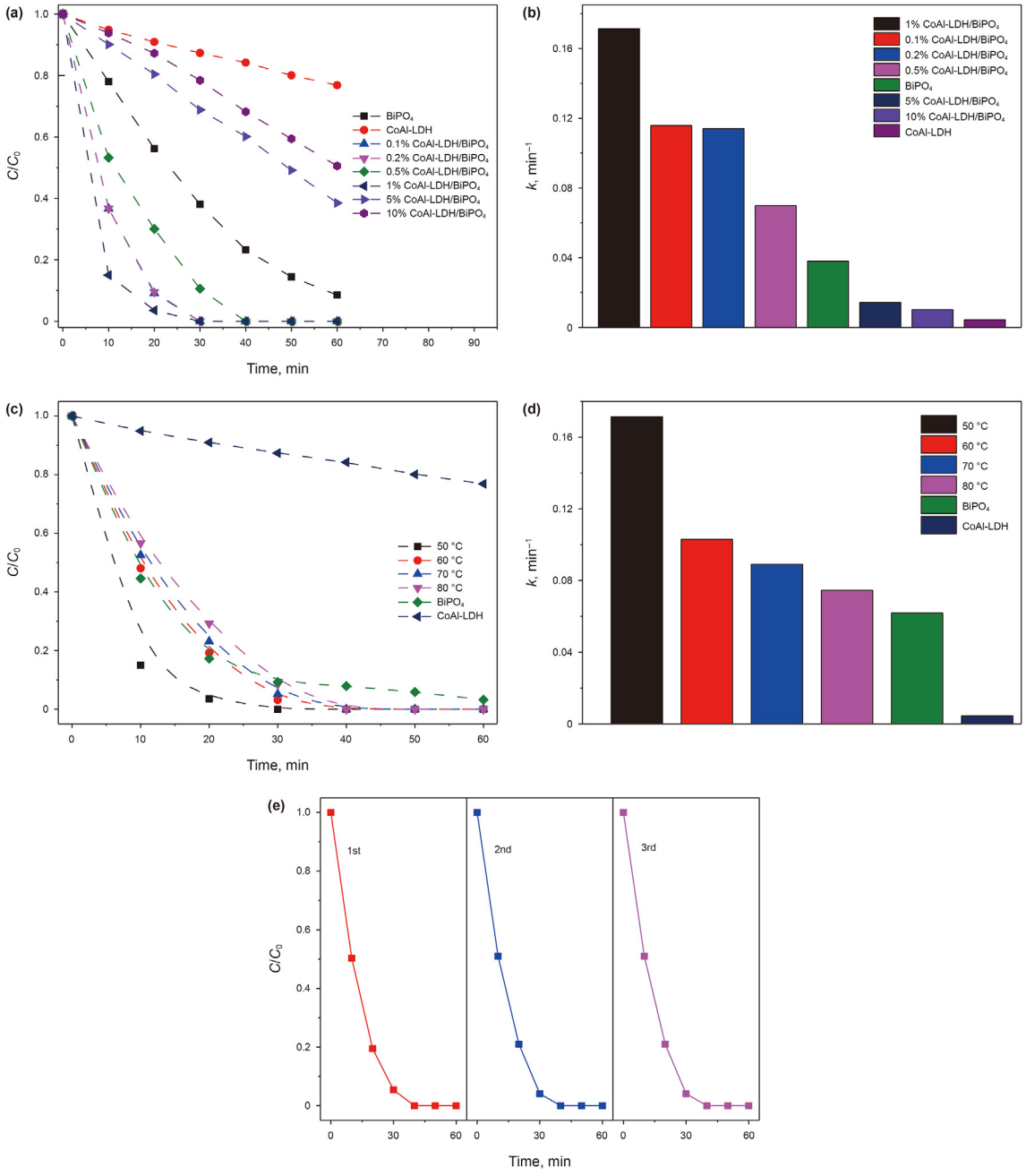

Fig. 3. Photocatalytic activities **a** and apparent rate constant *k* **b** of various CoAl-LDH/$BiPO_4$ composites; photocatalytic activities **c** and apparent rate constant *k* **d** of Co Al-LDH/$BiPO_4$ composites synthesized under different temperatures; **e** the degradation of phenol by 1% CoAl-LDH/$BiPO_4$ within successive three cycles (Experimental conditions: λ = 254 nm, [phenol] = 5 ppm, [catalyst] = 0.25 g/L, pH = 7, T = 25 °C).

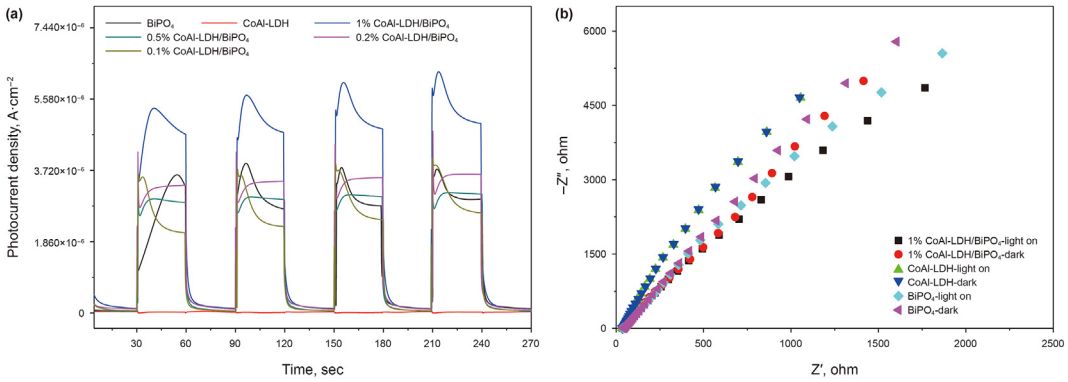

Fig. 4. **a** Photocurrent measurements of $BiPO_4$, CoAl-LDH and 1% CoAl-LDH/$BiPO_4$ under UV light radiation ($\lambda = 254$ nm); **b** EIS spectra of $BiPO_4$, CoAl-LDH and 1% CoAl-LDH/$BiPO_4$ in dark or under UV light radiation ($\lambda = 254$ nm).

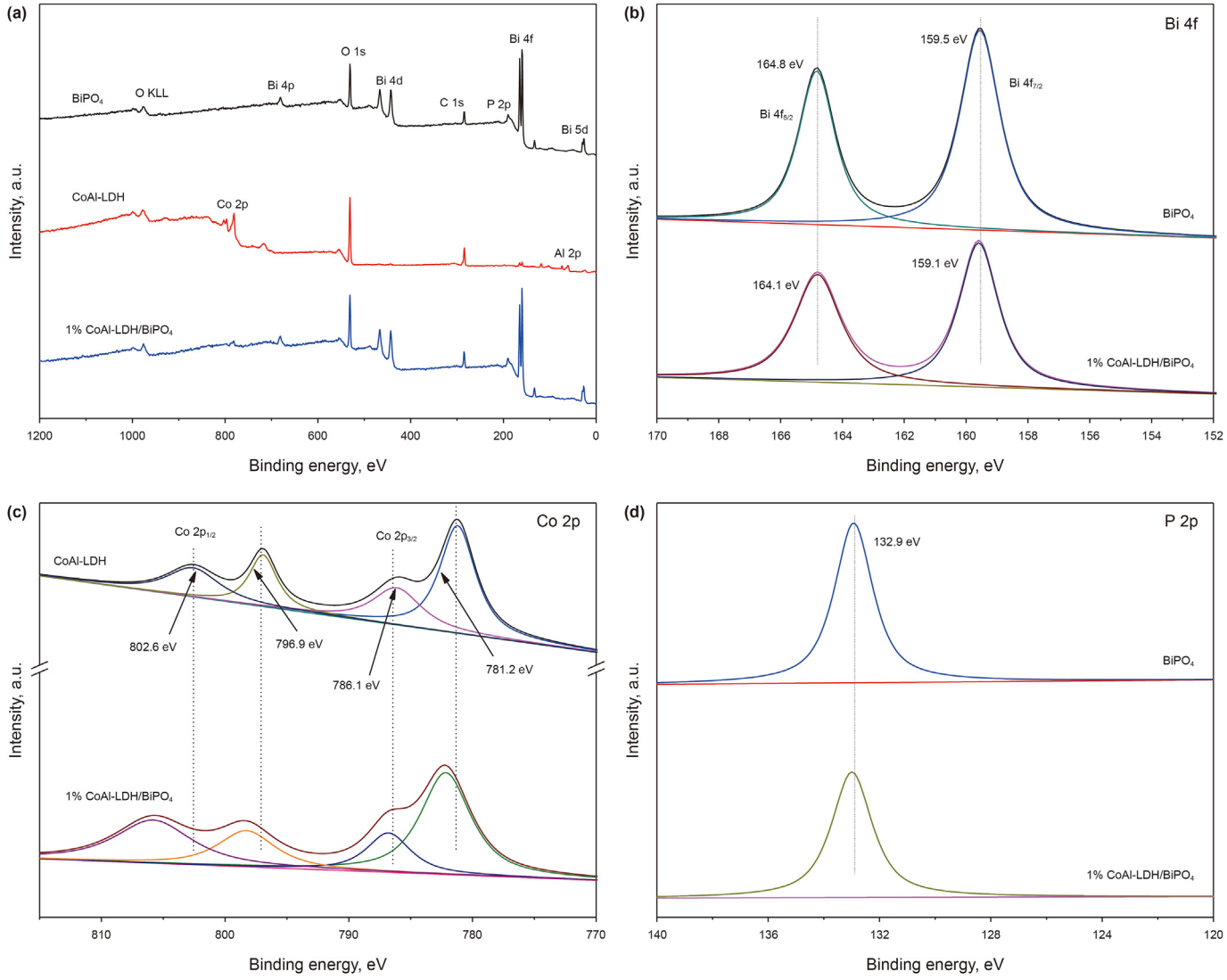

Fig. 5. **a** XPS spectra of $BiPO_4$, CoAl-LDH and 1% CoAl-LDH/$BiPO_4$; **b** Bi 4f spectra; **c** Co 2p spectra; **d** P 2p spectra.

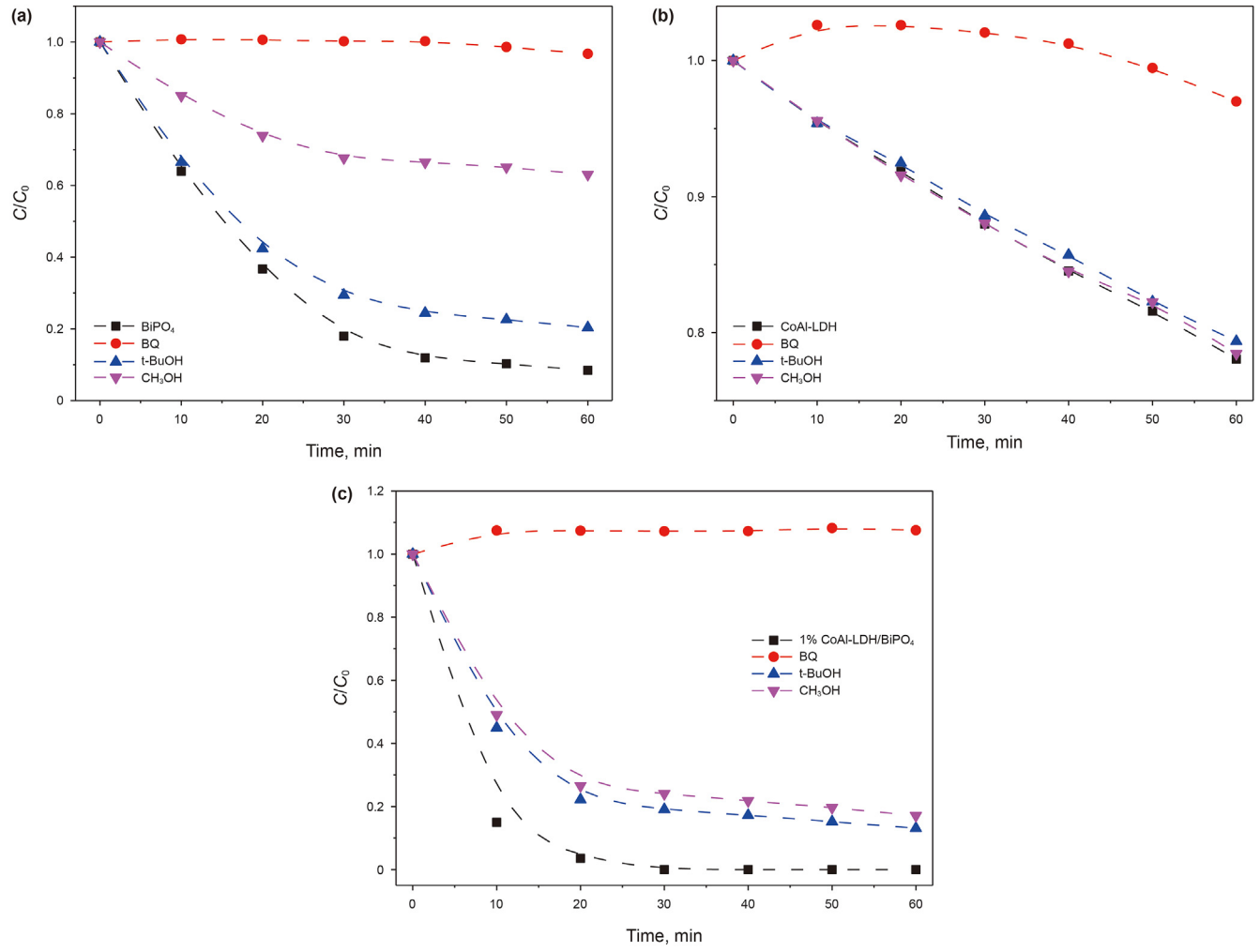

Fig. 6. Comparison of the photocatalytic performances of **a** $BiPO_4$, **b** CoAl-LDH and **c** 1% CoAl-LDH/$BiPO_4$ for the degradation of phenol without or with the addition of BQ, t-BuOH, or CH_3OH under UV light radiation ($\lambda = 254$ nm).

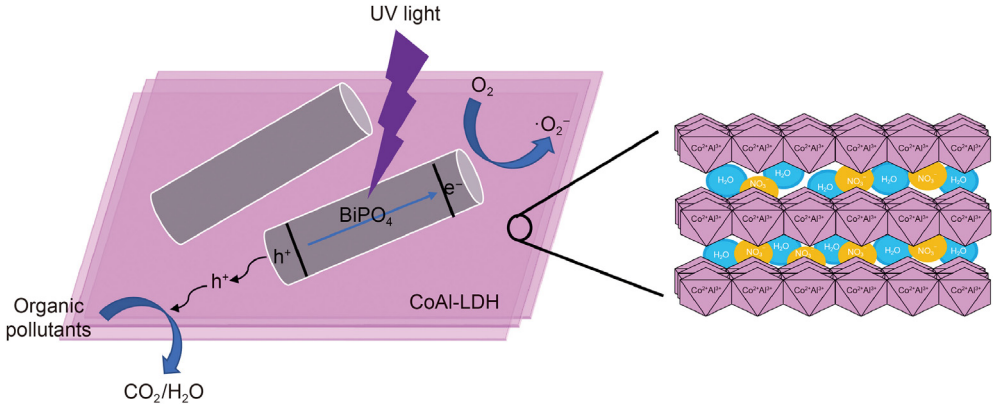

Fig. 7. The mechanism illustration of photocatalytic degradation of organics over CoAl-LDH/$BiPO_4$.

catalyst surface and react directly with pollutants. Therefore, in this system, the effective separation and transfer of photogenerated electron and hole pairs are the main reason for improving the activity of CoAl-LDH/$BiPO_4$.

4. Conclusion

We successfully synthesize high efficiency CoAl-LDH/$BiPO_4$ by hydrothermal and chemical adsorption. 1% CoAl-LDH/$BiPO_4$ shows significantly improved photocatalytic activity for phenol

degradation, which is about 3 times and 39 times higher than that of pure $BiPO_4$ and CoAl-LDH, respectively. In the degradation process, the main active species are $\cdot O_2^-$. In addition, 1% CoAl-LDH/$BiPO_4$ has superior stability and reusability in successive degradation cycles. Its excellent performance can be attributed to the rapid migration of photogenerated holes from $BiPO_4$ to CoAl-LDH, which improves the separation efficiency of photogenerated electron and hole pairs. This method is low-cost and easy to operate, which provides a new way to prepare $BiPO_4$ photocatalyst with high photocatalytic activity.

Acknowledgements

This work is supported by the National Key Research and Development Program of China [2019YFC1904500], National Natural Science Foundation of China [52270115, 21878331, 21777080] and Science Foundation of China University of Petroleum, Beijing [2462019QNXZ05, 2462020YXZZ018].

Appendix A. Supplementary data

Supplementary data to this article can be found online at https://doi.org/10.1016/j.petsci.2022.01.007.

References

Bacha, A.U.R., Nabi, I., Fu, Z.Y., Li, K.J., Cheng, H.Y., Zhang, L.W., 2019. A comparative study of bismuth-based photocatalysts with titanium dioxide for perfluorooctanoic acid degradation. Chin. Chem. Lett. 30 (12), 2225–2230. https://doi.org/10.1016/j.cclet.2019.07.058.

Cao, J., Xu, B.Y., Lin, L., Chen, S.F., 2013. Highly improved visible light photocatalytic activity of $BiPO_4$ through fabricating a novel p-n heterojunction BiOI/$BiPO_4$ nanocomposite. Chem. Eng. J. 228, 482–488. https://doi.org/10.1016/j.cej.2013.05.008.

Chen, Y.B., Li, J.F., Liao, P.Y., Zeng, Y.S., Wang, Z., Liu, Z.Q., 2020. Cascaded electron transition in $CuWO_4$/CdS/CDs heterostructure accelerating charge separation towards enhanced photocatalytic activity. Chin. Chem. Lett. 31 (6), 1516–1519. https://doi.org/10.1016/j.cclet.2019.12.013.

Chong, M.N., Jin, B., Chow, C.W., Saint, C., 2010. Recent developments in photocatalytic water treatment technology: a review. Water Res. 44, 2997–3027. https://doi.org/10.1016/j.watres.2010.02.039.

Chowdhury, S., Jiang, Y., Muthukaruppan, S., Balasubramanian, R., 2018. Effect of boron doping level on the photocatalytic activity of graphene aerogels. Carbon 128, 237–248. https://doi.org/10.1016/j.carbon.2017.11.089.

Di, J., Chen, J., Ji, M.X., Zhang, Q., Xu, L., Xia, J.X., Li, H.M., 2017. Reachable ionic liquid induced homogeneous carbon superdoping of $BiPO_4$ for superior photocatalytic removal of 4-chlorophenol. Chem. Eng. J. 313, 1477–1485. https://doi.org/10.1016/j.cej.2016.11.045.

Diego, C.B., Rafael, S., Damien, V., Tewodros, A., Manish, C., 2015. Copper nanoparticles stabilized by reduced graphene oxide for CO_2 reduction reaction. Mater Renew Sustain Energy 4, 2–7. https://doi.org/10.1007/s40243-015-0042-0.

Ding, K., Yu, D., Wang, W., Gao, P., Liu, B.J., 2018. Fabrication of multiple hierarchical heterojunction Ag@AgBr/$BiPO_4$/r-GO with enhanced visible-light-driven photocatalytic activities towards dye degradation. Appl. Surf. Sci. 445, 39–49. https://doi.org/10.1016/j.apsusc.2018.03.131.

Dou, Y., Zhang, S., Pan, T., 2015. TiO_2@ layered double hydroxide core-shell nanospheres with largely enhanced photocatalytic activity toward O_2 generation. Adv. Funct. Mater. 25, 2243–2249. https://doi.org/10.1002/adfm.201404496.

Fang, L.F., Evana, D.G., 2014. Catalytic applications of layered double hydroxides: recent advances and perspective. Chem. Soc. Rev. 43, 7040–7066. https://doi.org/10.1039/c4cs00160e.

Gao, L.G., Li, H.X., Song, X.L., Li, W.L., Ma, X.R., 2019. Degradation of benzothiophene in diesel oil by LaZnAl layered double hydroxide: photocatalytic performance and mechanism. Petrol. Sci. 16, 173–179. https://doi.org/10.1007/s12182-018-0285-3.

Gong, M., Dai, H., 2015. A mini review of NiFe-based materials as highly active oxygen evolution reaction electrocatalysts. Nano Res. 8, 23–39. https://doi.org/10.1007/s12274-014-0591-z.

Guo, Y., Wang, P., Qian, J., Ao, Y., Wang, C., Hou, J., 2018. Phosphate group grafted twinned $BiPO_4$ with significantly enhanced photocatalytic activity: synergistic effect of improved charge separation efficiency and redox ability. Appl. Catal. B Environ. 234, 90–99. https://doi.org/10.1016/j.apcatb.2018.04.036.

Huang, H.W., Qi, H.J., He, Y., Tian, N., Zhang, Y.H., 2013. Enhanced photocatalytic activity of Eu^{3+}- and Gd^{3+}-doped $BiPO_4$. J. Mater. Res. 28, 2977–2984. https://doi.org/10.1557/jmr.2013.296.

Ji, T.H., Yang, F., Lv, Y.Y., Zhou, J.Y., Sun, J.Y., 2009. Synthesis and visible-light photocatalytic activity of Bi-doped TiO_2 nanobelts. Mater. Lett. 63, 2044–2046. https://doi.org/10.1016/j.matlet.2009.06.043.

Jiang, J., Zhang, X., Sun, P.B., Zhang, L.Z., 2011. ZnO/BiOI heterostructures: photoinduced charge-transfer property and enhanced visible-light photocatalytic activity. J. Phys. Chem. C 115, 20555–20564. https://doi.org/10.1021/jp205925z.

Kumar, S., Isaacs, M.A., Trofimovaite, R., 2017. P25@CoAl layered double hydroxide heterojunction nanocomposites for CO_2 photocatalytic reduction. Appl. Catal. B Environ. 209, 394–404. https://doi.org/10.1016/j.apcatb.2017.03.006.

Lia, H.Y., Lia, J., Xua, C.C., Ping, Y.G., Dickon, H.L., Peng, S.G., Min, Z., 2017. Hierarchically porous MoS_2/CoAl-LDH/HCF with synergistic adsorption-photocatalytic performance under visible light irradiation. J. Alloys Compd. 698, 852–862. https://doi.org/10.1016/j.jallcom.2016.12.310.

Liu, Y.F., Zhu, Y.Y., Xu, J., Bai, X.J., Zong, R.L., Zhu, Y.F., 2013. Degradation and mineralization mechanism of phenol by $BiPO_4$ photocatalysis assisted with H_2O_2. Appl. Catal. B Environ. 142, 561–567. https://doi.org/10.1016/j.apcatb.2013.05.049.

Maisang, W., Phuruangrat, A., Randorn, C., Kungwankunakorn, S., Thongtem, S., Wiranwetchayan, O., Wannapop, S., Choopun, S., Kaowphong, S., Thongtem, T., 2018. Enhanced photocatalytic performance of visible-light-driven BiOBr/$BiPO_4$ composites. Mater. Sci. Semicond. Process. 75, 319–326. https://doi.org/10.1016/j.mssp.2017.11.002.

Mu, F.H., Dai, B.L., Zhao, W., Yang, X.F., Zhao, X.L., Guo, X.J., 2021. In-situ construction of amorphous/crystalline contact Bi_2S_3/Bi_4O_7 heterostructures for enhanced visible-light photocatalysis. Chin. Chem. Lett. 32 (8), 2539–2543. https://doi.org/10.1016/j.cclet.2020.12.016.

Naciri, Y., Hsini, A., Ajmal, Z., Navio, J.A., Bakiz, B., Albourine, A., Ezahri, M., Benlhachemi, A., 2020. Recent progress on the enhancement of photocatalytic properties of $BiPO_4$ using pi-conjugated materials. Adv Colloid Interfac 208, 102160. https://doi.org/10.1016/j.cis.2020.102160.

Pan, C.S., Zhu, Y.F., 2015. A review of $BiPO_4$, a highly efficient oxyacid-type photocatalyst, used for environmental applications. Catal. Sci. Technol. 5, 3071–3083. https://doi.org/10.1039/c5cy00202h.

Pellegrino, F., Morra, E., Mino, L., Martra, G., Chiesa, M., Maurino, V., 2020. Surface and bulk distribution of fluorides and Ti^{3+} species in TiO_2 nanosheets: implications on charge carrier dynamics and photocatalysis. J. Phys. Chem. C 124, 3141–3149. https://doi.org/10.1021/acs.jpcc.9b10912.

Santosh, K., Mark, A.I., Rima, T., Lee, D., Christopher, M.A., Richard, E.D., Ben, C., Martin, C.R., Karen, W., Adam, F.L., 2017. P25@CoAl layered double hydroxide heterojunction nanocomposites for CO_2 photocatalytic reduction. Appl. Catal. B Environ. 209, 394–404. https://doi.org/10.1016/j.apcatb.2017.03.006.

Santosh, K., Lee, J.D., Jinesh, C.M., Mark, A.I., Christopher, M.A., Sekar, K., Richard, E.D., Ben, C., Karen, W., Adam, F.L., 2018. Delaminated CoAl-layered double hydroxide@TiO_2 heterojunction nanocomposites for photocatalytic reduction of CO_2. Part. Part. Syst. Char. 35, 1700317. https://doi.org/10.1002/ppsc.201700317.

Shekofteh, G.M., Habibi, Y.A., Abitorabi, M., Rouhi, A., 2018. Magnetically separable nanocomposites based on ZnO and their applications in photocatalytic processes: a review. Crit. Rev. Environ. Sci. Technol. 48, 806–857. https://doi.org/10.1080/10643389.2018.1487227.

Shi, J.Z., Meng, X.Y., Hao, M.J., Cao, Z.Z., He, W.Y., Gao, Y.F., Liu, J.R., 2018. Enhanced photoactivity of $BiPO_4$/(001) facet-dominated square BiOBr flakes by combining heterojunctions with facet engineering effects. J. Phys. Chem. Solid. 113, 142–150. https://doi.org/10.1016/j.jpcs.2017.10.031.

Shi, J.L., Chen, R.F., Hao, H.M., Wang, C., Lang, X.J., 2020. 2D sp^2 carbon-conjugated porphyrin covalent organic framework for cooperative photocatalysis with TEMPO. Angew. Chem. Int. Ed. 59 (23), 9088–9093. https://doi.org/10.1002/anie.202000723.

Snehaprava, D., Sulagna, P., Parida, K.M., 2019. Fabrication of a Au-loaded $CaFe_2O_4$/CoAl LDH p-n junction based architecture with stoichiometric H_2 & O_2 generation and Cr(VI) reduction under visible light. Inorg. Chem. Front. 6, 94–109. https://doi.org/10.1039/C8QI00952J.

Su, Y.N., Tan, G.Q., Liu, T., Lv, L., Wang, Y., Zhang, X.L., Yue, Z.W., Ren, H.J., Ao, X., 2018. Photocatalytic properties of Bi_2WO_6/$BiPO_4$ Z-scheme photocatalysts induced by double internal electric fields. Appl. Surf. Sci. 457, 104–114. https://doi.org/10.1016/j.apsusc.2018.06.153.

Vadivel, S., Naveen, A.N., Theerthagiri, J., 2016. Solvothermal synthesis of $BiPO_4$/MWCNT (1D-1D) composite for photocatalyst and supercapacitor applications. Ceram. Int. 42, 14196–14205. https://doi.org/10.1016/j.ceramint.2016.05.080.

Wan, K.J., Surendar, T., 2019. Novel CoAl-LDH/g-C_3N_4/RGO ternary heterojunction with notable 2D/2D/2D configuration for highly efficient visible-light-induced photocatalytic elimination of dye and antibiotic pollutants. J. Hazard Mater. 368, 778–787. https://doi.org/10.1016/j.jhazmat.2019.01.114.

Wang, Q., O'hare, D., 2012. Recent advances in the synthesis and application of layered double hydroxide (LDH) nanosheets. Chem. Rev. 112, 4124–4155. https://doi.org/10.1021/cr200434v.

Wang, Y.J., Shi, R., Lin, J., Zhu, Y.F., 2011. Enhancement of photocurrent and photocatalytic activity of ZnO hybridized with graphite-like C_3N_4. Energy Environ. Sci. 4, 2922–2929. https://doi.org/10.1039/C0EE00825G.

Wang, L., Wang, N., Wang, S., Liang, D., Cai, X., Wang, D., Jia, G., 2018. Preparation of lanthanide ions-doped $BiPO_4$ nanoparticles and Fe^{3+} ions assay. J. Nanosci. Nanotechnol. 18, 4000–4005. https://doi.org/10.1166/jnn.2018.15038.

Wang, H.J., Zhang, J., Wang, P., Yin, L.L., Tian, Y., Li, J.J., 2020. Bifunctional copper modified graphitic carbon nitride catalysts for efficient tetracycline removal: synergy of adsorption and photocatalytic degradation. Chin. Chem. Lett. 31 (10), 2789–2794. https://doi.org/10.1016/j.cclet.2020.07.043.

Wang, Y.J., Liu, L.M., Zhang, J.Y., Zhang, W.C., Yao, W.Q., Jiang, G.Y., 2021. NiFe-layered double hydroxide/vertical Bi_2WO_6 nanoplate Arrays with oriented {001} facets supported on ITO glass: improved photoelectrocatalytic activity and mechanism insight. ChemCatChem 13, 3414–3420. https://doi.org/10.1002/cctc.202100166.

Yi, J.J., Li, H.P., Gong, Y.J., She, X.J., Song, Y.H., Xu, Y.G., Deng, J.J., Yuan, S.Q., Xu, H., Li, H.M., 2019. Phase and interlayer effect of transition metal dichalcogenide cocatalyst toward photocatalytic hydrogen evolution: the case of $MoSe_2$. Appl. Catal. B Environ. 243, 330–336. https://doi.org/10.1016/j.apcatb.2018.10.054.

Yu, Z.D., Wang, D.H., Xun, S.H., He, M.Q., Ma, R.L., Jiang, W., Li, H.P., Zhu, W.S., Li, H.M., 2018. Amorphous TiO_2-supported Keggin-type ionic liquid catalyst catalytic oxidation of dibenzothiophene in diesel. Petrol. Sci. 15, 870–881. https://doi.org/10.1007/s12182-018-0268-4.

Zeng, H.X., Zhang, H.J., Deng, L., Zhou, S., 2020. Peroxymonosulfate-assisted photocatalytic degradation of sulfadiazine using self-assembled multi-layered CoAl-LDH/g-C_3N_4heterostructures: performance, mechanism and eco-toxicity evaluation. J. Water Proc. Eng. 33, 101084. https://doi.org/10.1016/j.jwpe.2019.101084.

Zhang, H., Lv, X.J., Li, Y.M., Wang, Y., Li, J.H., 2010. P25-graphene composite as a high performance photocatalyst. ACS Nano 4, 380–396. https://doi.org/10.1021/nn901221k.

Zheng, Y.J., Wang, X.D., Cui, L.S., 2010. Synthesis of ZnS from organic sulfur in petroleum coke and its photocatalysis properties. Petrol. Sci. 7, 268–272. https://doi.org/10.1007/s12182-010-0032-x.

Zhu, Y.Y., Wang, Y.J., Ling, Q., Zhu, Y.F., 2017. Enhancement of full-spectrum photocatalytic activity over $BiPO_4/Bi_2WO_6$ composites. Appl. Catal. B Environ. 200, 222–229. https://doi.org/10.1016/j.apcatb.2016.07.002.

Zou, X., Dong, Y., Zhang, X., Cui, Y., Ou, X., Qi, X., 2017. The highly enhanced visible light photocatalytic degradation of gaseous o-dichlorobenzene through fabricating like flowers $BiPO_4$/BiOBr pn heterojunction composites. Appl. Surf. Sci. 391, 525–534. https://doi.org/10.1016/j.apsusc.2016.06.003.